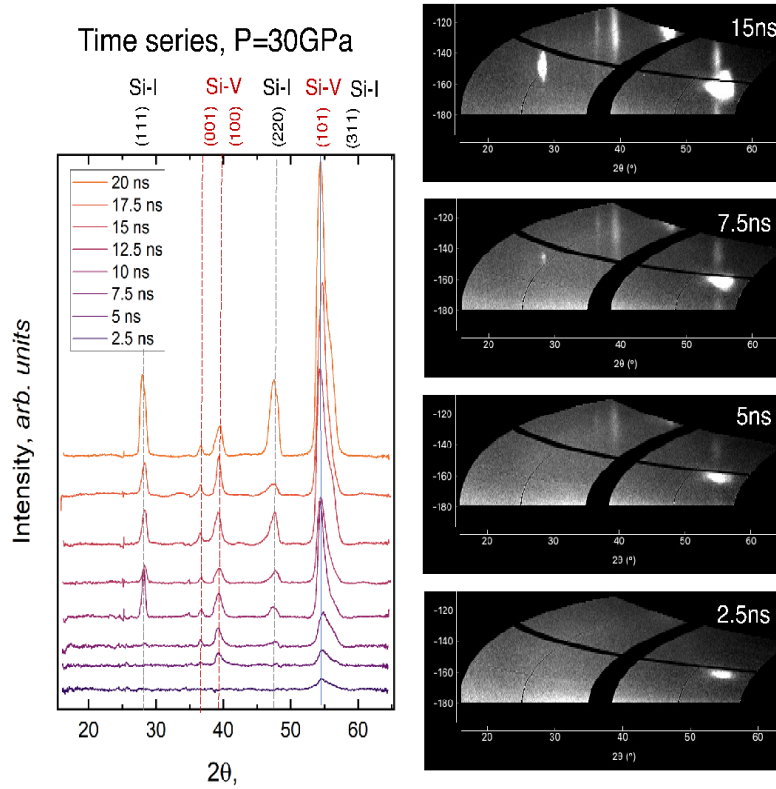
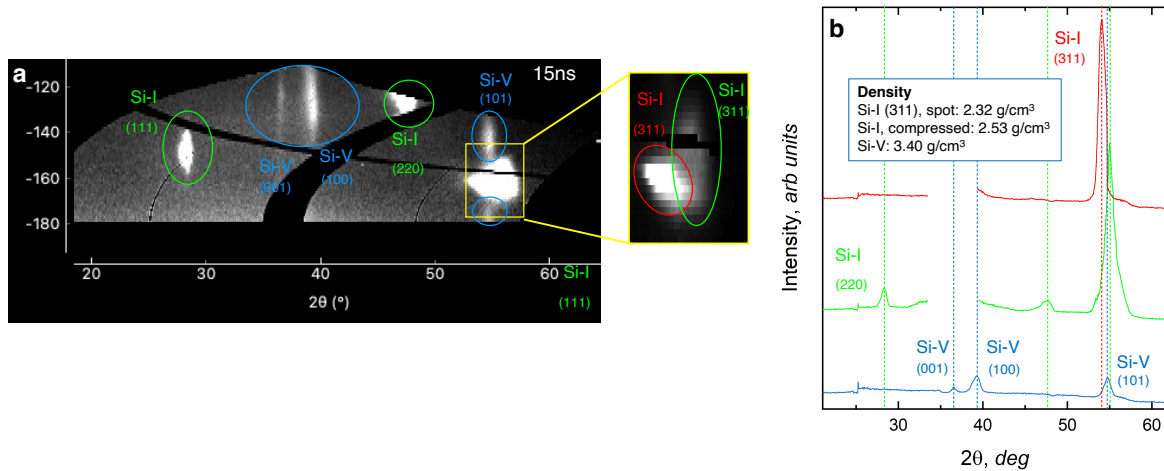


## Supplementary Information file:



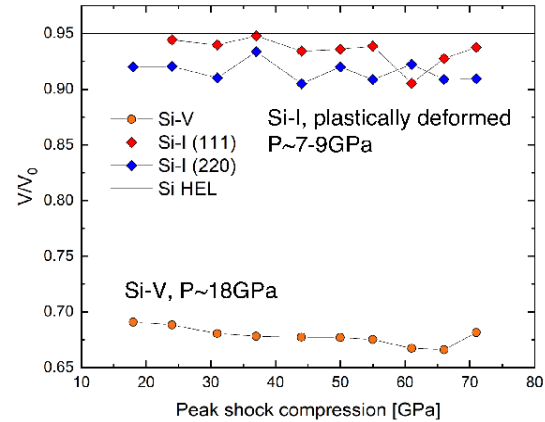
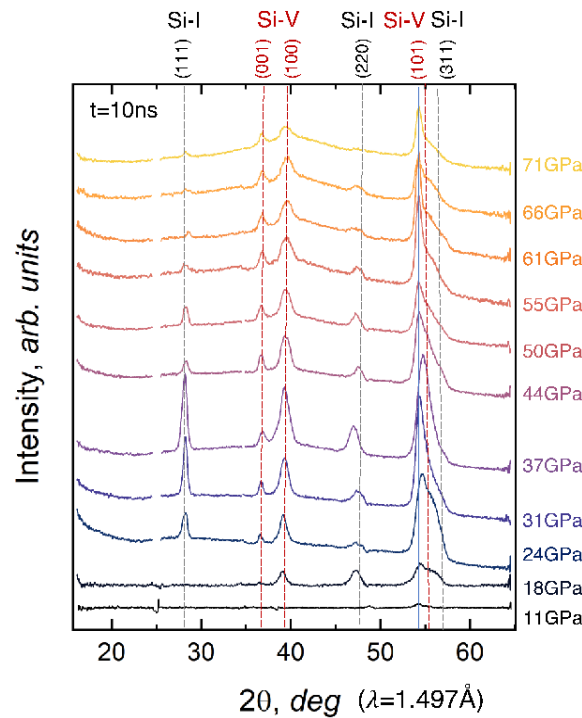
**Supplementary Figure 1.**  
**Left:** azimuthally integrated X-ray Diffraction data acquired at 30 GPa peak pressure at different time delays. The peaks from both the compressed Si-I and the high-pressure phase, Si-V, are indexed, and their position does not vary appreciably over time; the intensity and width of the peaks, on the contrary, changes as the compressed portion of the sample increases; in particular, the intensity and width of the peak at  $\sim 55^\circ$  increase considerably.



**Supplementary Figure 2.**

**a:** XRD data projected onto the scattering-azimuthal angle plane; peaks from different phases are indexed and highlighted using different colors. The peaks corresponding to the (311) reflection of the starting Si-I are highlighted in green and red depending whether they come from the compressed or uncompressed portion of the sample, respectively.

**b:** azimuthally integrated pattern of spatially selected data. The portion of the 2D image to analyze for each pattern has been chosen as to select only one phase for each pattern, as shown on the left; the data is plotted with the same colors used in the panel **a**. It is clear that, especially for the peaks around 55°, this spatial filtering allows us to clearly evaluate the position of the peaks corresponding to each phase, and thus correctly evaluate its density. The values obtained for each phase are also reported.

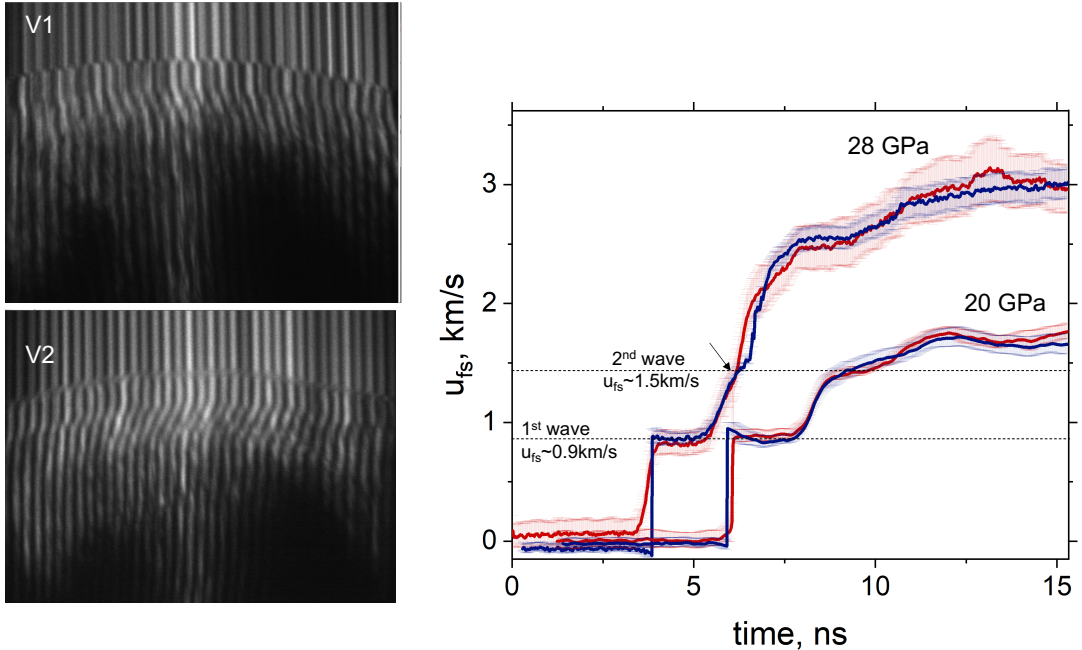


**Supplementary Figure 3.**

Right: integrated XRD data at increasing pressure. The peaks of both Si-I and Si-V phases are indexed, and the pressure estimated from VISAR measurements is reported for each pattern. As the XRD data comes from the whole imaged area, we see that the signature of the mixed V/I phase does not change appreciably; on the other hand, at higher pressures the peaks become less prominent and

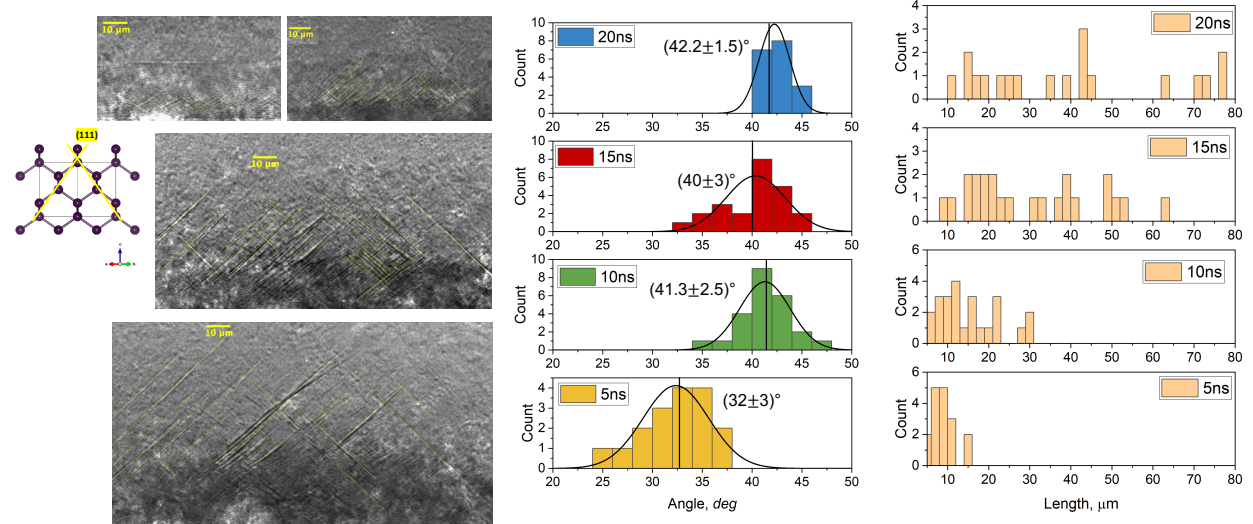
broader and the background increases as most of the sample (behind the phase transition front) is in the molten state.

**Left:** density calculated from the crystalline portion of the sample, *i.e.*, the Si-V and compressed Si-I bands; the density does not vary appreciably in that region of the sample at varying peak pressure.



**Supplementary Figure 4.**

**Left.** representative velocimetry data (for both arms) collected on silicon **Right.** extracted free surface velocity profile. The pressure has also been estimated using data from the Kapton-LiF interface at different energies to calculate ablation pressure, and the correspondent pressure in silicon has been calculated via impedance-matching.

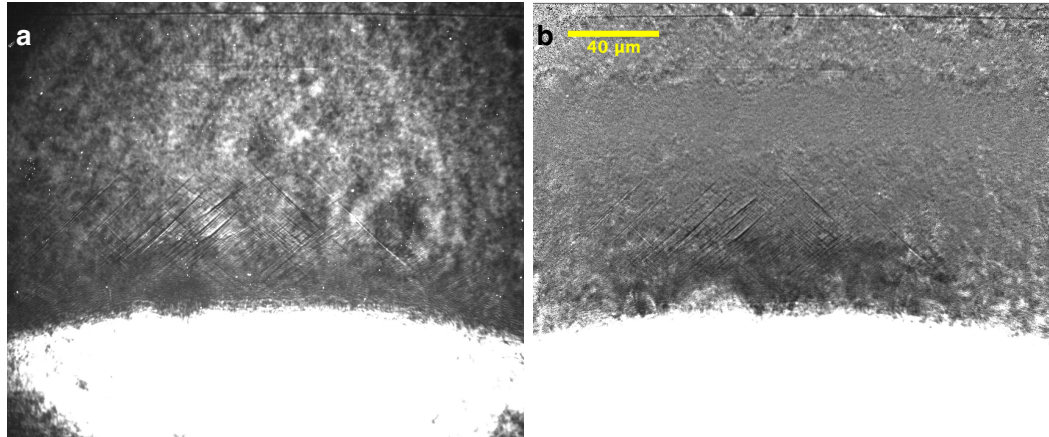


**Supplementary Figure 5.**

**Right:** zoomed view of X-ray images acquired at 30 GPa at different time delays; the line overlaid to the figures show the bands analyzed for assessing length and orientation variation.

**Center:** histograms of the bands' orientation at varying time delays as estimated from the images. The angles are measured with respect to the horizontal direction in the figure (*i.e.*, the (110) crystal axis in the starting material), and the statistical analysis is performed on the angles' absolute values.

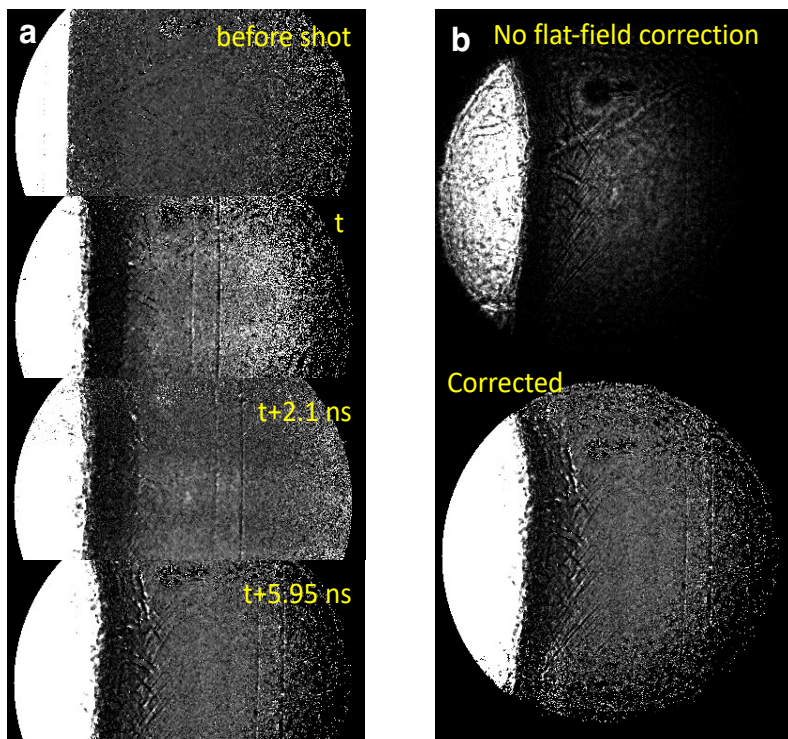
**Right:** histograms of the bands' length, expressed in  $\mu\text{m}$ , at varying time delays.



**Supplementary Figure 6.**

**Left:** raw X-ray image

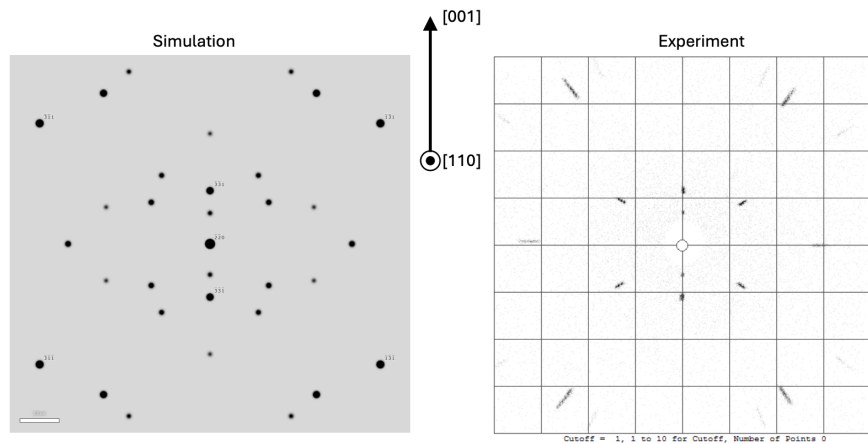
**Right:** flat-field corrected image, with highly improved visibility. For more details on the procedure, see Method section.



**Supplementary Figure 7.**

**a.** representative sequence of images collected using the UXI camera and the four-pulse mode at LCLS. All images are flat-field corrected. The top image was collected before launching the shock wave, while the three frames collected during the shock-wave propagation were collected at fixed temporal intervals (*i.e.*, 2.1 ns between the first and the second frame, and 3.85 ns between the second and third one).

**b.** representative results from the flat-field correction procedure for the UXI images. The top panel shows the raw image, while the bottom one presents the corrected image, with improved visibility.



## Supplementary Figure 8.

Simulated (Left) and experimental (Right) XRD data of the starting Si-I material; nominal orientation was confirmed: the drive laser compressed along the [001] direction, while the XFEL beam probes along the [110] direction.